

A PROPOSAL FOR ENHANCING TECHNOSIGNATURE SEARCH TOWARD THE GALACTIC CENTER

NAOKI SETO

Department of Physics, Kyoto University, Kyoto 606-8502, Japan
Draft version April 2, 2024

ABSTRACT

We discuss the possibility of enhancing intelligent life searches toward the Galactic center. From the clockwork orbital motions of stars around the Sgr A* black hole, we can determine the distance to the Galactic center at an exceptional accuracy, despite its remoteness ~ 8.3 kpc. In addition, we can define precise reference epochs by selecting a prominent object such as the bright B-type star S2. These properties have a particular affinity for the coordinated signaling scheme that was hypothesized by Seto (2019) for systematically connecting intentional senders to searchers without a prior communication. If S2 is actually being used as a common reference clock, we can compress the search directions around the Galactic center by more than 2 orders of magnitude, with the scanning interval of ~ 16 yr.

Subject headings: extraterrestrial intelligence —astrobiology —Galaxy: center

1. INTRODUCTION

In our Galaxy, an extraterrestrial intelligence (ETI) might intentionally transmit artificial signals to other unknown civilizations. However, in spite of our intermittent searches over the past 60 yr (Drake 1961; Tarter 2001; Siemion, et al. 2013; Lingam & Loeb 2021), we have not succeeded a definite detection yet. While the number of Galactic intentional senders is totally unclear, our observational and computational resources might be too deficient to examine the vast parameter combinations that potentially contain ETI signals (Tarter et al. 2010; Wright et al. 2018). In the meantime, there might be tacit adjustments between the senders and receivers to compress the parameter space (Wright 2018). Such adjustments will be beneficial to both parties for saving various investments, including the antennas for signal transmissions and receptions, the electric power for outgoing signals and data analysis, and so on.

In the game theory, Schelling (1960) made a pioneering work on tacit adjustments without prior communications. The resultant choice is called the Schelling point. Here, uniqueness, prominence, and symmetry are considered to be key at converging the adjustments. In fact, some aspects of ETI search have been discussed in relation to the Schelling point (already mentioned in Schelling 1960 about the work by Cocconi & Morrison 1959, see also Pace & Walker 1975; McLaughlin 1977; Makovetskii 1980; Kipping & Teachey 2016; Wright 2018). In this context, the author recently pointed out that a coordinated signaling scheme (hereafter the concurrent signaling scheme) might be prevailing in the Galaxy (Seto 2019). Through a common usage of a conspicuous astronomical event, this scheme allows both senders and receivers to limit the target sky directions, without depending on their mutual distances (see also Nishino & Seto 2018).

In the concurrent scheme, for narrowing down the search directions, we need to precisely estimate both the three-dimensional position and the epoch of the reference event. The author proposed to use a future binary neutron star merger for the scheme (Seto 2019) and past supernova (SN) explo-

sions for an extended version (Seto 2021). However, as explained later, these candidates currently have shortcomings at actual applications.

Meanwhile, the Galactic center is a salient place in our island Universe (see, e.g. Binney & Merrifield 1998). Partly motivated by its specialty, ETI signals have indeed been searched around the direction of the Galactic center (Shostak & Tarter 1985; Worden et al. 2017; Gajjar et al. 2021; Tremblay et al. 2022; Suresh et al. 2023). Importantly, by observing nearly regular orbital motions of stars around the massive black hole there, we can determine the distance l_H to the Galactic center at an exceptional precision, in spite of its remoteness ~ 8.3 kpc (GRAVITY Collaboration et al. 2019, 2021). Furthermore, we can set a sequence of reference epochs at high precision, for example, by using the pericenter passages of a prominent star such as the bright B-type star S2 (GRAVITY Collaboration et al. 2019, 2021). These properties are highly preferable for applying the concurrent signaling scheme around the direction of the Galactic center. In this paper, we discuss this possibility, by concretely setting S2 as the reference clock.

This paper is organized as follows. In section 2, we explain the basic idea of the concurrent signaling scheme and its extension. We mention drawbacks of a binary neutron star merger and an SN explosion, which were proposed as conspicuous reference events in the previous works. In section 3, we argue the primary aspects of the Galactic center, in relation to the concurrent signaling scheme. In section 4, we evaluate the expected search directions, using the timing information of S2. In section 5, we discuss the relaxation effects for the long-term regularity of S2's orbit. In section 6, we discuss issues relevant to our study. Section 7 is devoted to a short summary. In the appendix, we discuss correction effects such as the aberration of light. Throughout this paper, we assume that the intentional signals propagate at the speed of light c .

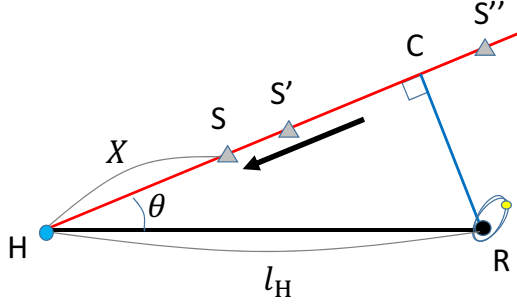


FIG. 1.— Schematic picture for the concurrent signaling scheme. The senders S , S' and S'' on the red line can synchronize their signal propagation so that their transmissions propagate synchronously with an imaginary photon that has passed the closest approach C (to the reference point R) when the event occurs. The receiver H can concurrently receive the intentional signals (from the senders S , S' and S'') irrespective of the mutual distances. We put X as the distance between the receiver H and the sender S .

2. CONCURRENT SIGNALING SCHEME

2.1. basic idea

We first explain the basic idea of the concurrent signaling scheme (Seto 2019). As its building block, we can consider signal transmissions along a given oriented straight line (indicated in red in Fig. 1). Our goal is to synchronize the signal transmissions for all the senders on the line. To determine the sending time at each point on the line, we use a conspicuous astronomical event (e.g. an energetic burst) as a common reference. For each sender, the reference event needs to be observed in future and should be selected on the ground that both its position R and epoch can be estimate beforehand at high precision. In the next subsection, we discuss a binary neutron star merger as a potential candidate for a reference event.

In three-dimensional space, for an arbitrary combination of a line and an external reference point R , the closest approach C will be the unique point selected as the Schelling point (see Fig. 1). Then, we can synchronize the signal transmission along the oriented line so that the emitted signals pass the close approach C at the time of the burst occurrence. We illustrate the time sequence of the signal propagation in Fig. 2. Strictly speaking, among the senders S , S' and S'' in Fig. 1, only the signals of the sender S'' (upstream of the point C) can pass the point C . But the remaining senders S and S' (downstream of C) can easily know the appropriate epochs for their signal transmissions along the oriented line (see panel (c) in Fig. 2). Note that, in the present scheme, a sender should receive upstream signals, at the time of transmitting its own intentional signals (toward the antipodal direction). On the red line in Fig. 2, at each epoch, the position of the intentional signal (blue arrow) is identical to the position of the sender.

Next, as an example, we consider an ETI searcher H at the distance l_H from the reference. We discuss how its receiving directions change with time. At the time $2l_H/c$ before observing reference event, the receiving direction is $\theta = \pi$ in Fig. 1 (considering the limit $\lim RC \rightarrow 0$). Similarly, just at observing the reference event, the receiving direction is $\theta = 0$. In the time between, the receiving directions are on a circle in the sky, centered by the reference direction. Its opening angle θ can be determined as a function of time (presented later in Section 4 with the parameter $q = 0$), only from the information of the reference. In this manner, the concurrent signaling

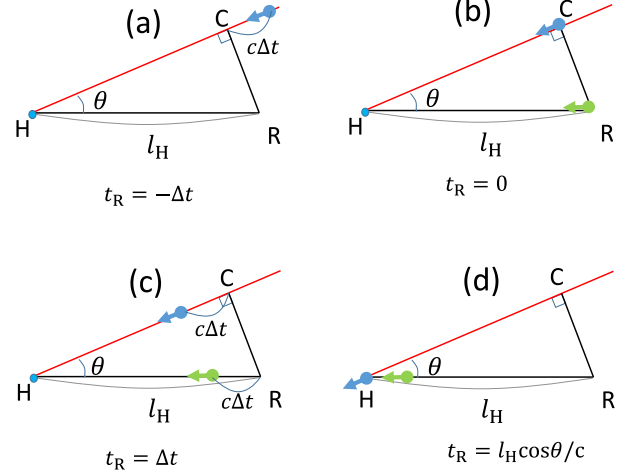


FIG. 2.— The time series of the signaling scheme with $q = 0$. We put $t_R = 0$ at the time of the reference event. The blue arrow shows the propagation position of the intentional signals and is identical to the position of the sender at the time. The green arrow shows the position of the photons marking the reference event. At the time $t_R < 0$, the intentional signal is at the upstream of the close approach C (panel (a)). The intentional signal reaches C at $t_R = 0$ (panel (b)). With $CH < RH$, the intentional signal is observed earlier than the photons of the reference event (panel (d)).

scheme is simple and enables involved civilizations to largely compactify the sending and receiving sky directions, irrespective of their mutual distances.

2.2. Reference Events

As mentioned in the previous subsection, for the common reference, we need to select a future astronomical event. Its position and epoch must be predicted beforehand at high precision. As a candidate of such a reference in our Galaxy, Seto (2019) proposed a binary neutron star merger (at a typical distance $l_H \sim 10\text{kpc}$) with the observed orbital frequency $\sim 1.5\text{mHz}$. From the first principles of physics, by using the planned Laser Interferometer Space Antenna (LISA; Amaro-Seoane et al. 2017) for ~ 10 yr, its distance l_H can be determined at subpercent level with relatively negligible error for the arrival epoch of the merger signal (Seto 2019). However, LISA is unlikely to be launched before the mid-2030s. In addition, we might not have a suitable neutron star binary in our Galaxy, given the decline of the estimated co-moving merger rate by the LIGO-Virgo-Kagra collaboration in the past 4 yr (Abbott et al. 2021). More specifically, there might be no neutron star binary whose merger signal will arrive to us in the time $2l_H/c$ from now. It is thus interesting to think about other references and/or possible extensions of the scheme.

For the original scheme in Seto (2019), we need to use a reference astronomical event that will be observed in the future. As an alternative choice for the synchronized passage time (of the intentional signals) at the point C , Seto (2021) proposed the epoch when the reference event signal reaches the point C (namely, RC/c later than the original epoch with $q = 0$). Then, from the triangular inequality in Fig. 1

$$RH < RC + CH, \quad (1)$$

we can receive (and send) intentional signals after observing the reference astronomical event. In Section 4, this extension will be analyzed with the parameter $q = 1$.

While the additional complexity will not be preferred for the tacit adjustment, this post-factum nature enables us to use historical SN explosions recorded in the past ~ 2000 yr, as potential references for the concurrent scheme. Seto (2021) provided the receiving sky directions associated with five SNe whose remnants are relatively well identified. Using Gaia data, Nilipour et al. (2023) actually examined potential ETI signals for some of the predicted directions (also adding the case for SN1987).

Unfortunately, even though the arrival times of the SN signals are well determined from the historical records, their distances typically have large uncertainties (e.g. 20% for the Crab pulsar associated with SN1054; see Kaplan et al. 2008). Consequently, the angular width $\Delta\theta$ of the receiving circle becomes large and the compactification of the directional parameters is limited.

3. GALACTIC CENTER

The Galactic center is a cynosure place in the Milky Way, and the surface density of stars is highly enhanced around its sky position (Binney & Merrifield 1998). In consideration of these aspects, ETI signals have been searched around the direction of the Galactic center (Shostak & Tarter 1985; Worden et al. 2017; Gajjar et al. 2021; Tremblay et al. 2022; Suresh et al. 2023). Notably, in relation to the concurrent signaling scheme, the distance to the Galactic center (more precisely Sgr A*) is measured at an exceptional accuracy despite its remoteness (GRAVITY Collaboration et al. 2019, 2021). This measurement is based on the nearly clockwork orbital motions of stars around the massive black hole there. For a given orbital period (e.g. 10yr), because of its extraordinary mass ($\sim 4.2 \times 10^6 M_\odot$), the Sgr A* black hole swings nearby stars at much larger spatial scale, compared with ordinary main-sequence star binaries. Thus, the combination of their radial velocities and the proper motions allows us to make a high-precision measurement of the distance l_H , on the basis of the simple orbital dynamics. Indeed, using the Very Large Telescope Interferometer, GRAVITY Collaboration et al. (2021) recently reported

$$l_H = 8275 \pm 9_{\text{stat}} \pm 33_{\text{sys}} \text{ pc.} \quad (2)$$

How about the reference time of the Galactic center for our signaling scheme? Here the nearly regular orbital motions of the stars will be very useful. For each star, a pericenter passage time will be the primary candidate for the reference epoch. In fact, because of the regularity of an orbit, we can calculate the sequence of its passage times both in the past and future directions. Note that, compared with an apocenter passage, a pericenter passage has a more drastic orbital variation, in particular for a highly eccentric orbit.

However, it is not obvious which star in the cluster we should choose for a reference. Here, from a surveillance of relevant research activities by human beings in the past ~ 20 yr (see, e.g. Eckart & Genzel 1996; Schödel et al. 2002; Ghez et al. 2003; Genzel et al. 2010; Bland-Hawthorn & Gerhard 2016), we select the B-type star S2, which is regarded as the most prominent star for its luminosity and orbital period. In addition, the formation scenario of this bright star was actually puzzling at its discovery (Ghez et al. 2003). At the solar system barycenter (SSB), this star has the most recent pericenter passage at

$$t_0 = 2018.378990 \pm 0.000082 \text{ yr} \quad (3)$$

with the estimated orbital period

$$P_0 = 16.0458 \pm 0.00013 \text{ yr} \quad (4)$$

and a high eccentricity $e = 0.8842$ (GRAVITY Collaboration et al. 2021).

Our choice of S2 is partly for concrete demonstration of the scheme and might be also useful for starting reanalysis on the already obtained SETI data around the Galactic center direction. However, we should be open-minded to consider the possible references other than S2, in particular intriguing objects uncovered in the years to come.

4. SEARCH DIRECTIONS

We now evaluate the opening angle θ of the receiving direction around the Galactic center ($\alpha = 17\text{h}46\text{m}40\text{s}$, $\delta = -29^\circ 0' 28''$), with the time reference determined by the pericenter passages of S2. We first explain the parameter q defined for the choice of the passage time of intentional signals at the closest approach C in Fig. 1. As already mentioned in Sections 2.1 and 2.2, the parameter q specifies the epoch when the intentional signals pass the closest approach C. For the original choice $q = 0$, the epoch is identical to the occurrence of the reference event. For $q = 1$, the epoch is when the photons of the reference event reach the point C (i.e. RC/c later than the choice $q = 0$).

In terms of the timing parameters t_0 and P_0 of S2, we can approximately put the epochs of its future and past pericenter passages (observed at the SSB) by

$$t_n \simeq t_0 + P_0 n \quad (5)$$

with the integers $n \leq 0$ for the past ones (related to $q = 1$) and $n \geq 1$ for the future ones (related to $q = 0$). For a given n , we estimate the opening angle θ_n of the receiving cones, as functions of the data taking epoch t_d . Below, we collectively deal with different n . If this abstract treatment looks confusing, one can fix the integer n at a specific value (e.g. $n = 2$ automatically with $q = 0$).

For each passage time t_n , we take into account the photon travel times for the distances ER, CE, and RC (only for $q = 1$) shown in Fig. 1. We obtain the condition for θ_n

$$t_d = t_n - l_H/c + l_H \cos \theta_n/c + q l_H \sin \theta_n/c \quad (6)$$

or equivalently

$$(1 - \cos \theta_n - q \sin \theta_n) = f n - f(t_d - t_0)/P_0 \quad (7)$$

Here we define the ratio

$$f \equiv \frac{P_0 c}{l_H} \quad (8)$$

with $f = 6.02 \times 10^{-4}$ for S2 (GRAVITY Collaboration et al. 2021).

Next, just for roughly showing the dependence on n , we put $t_d = t_0$ and solve Eq. (7), assuming $\theta_n \ll 1$. For the original scheme with $q = 0$, we obtain

$$\theta_n \sim \sqrt{2nf} \quad (9)$$

with $n > 0$. Meanwhile, for the modified version with $q = 1$, we obtain

$$\theta_n \sim |n|f \quad (10)$$

with $n \leq 0$.

For a moderate magnitude $|n|$ (e.g. $\lesssim 10$), we can have a much larger angle θ_n with the original choice $q = 0$ than the extended one $q = 1$. Also considering the lucidity of the original method, we mainly discuss the choice $q = 0$ ($n > 0$)

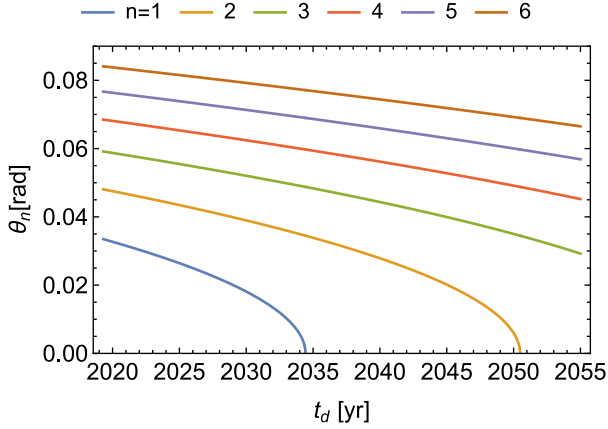


FIG. 3.— The opening angles θ_n for the receiving cones with $q=0$ around the direction to the Galactic center. For the reference time, we use the periastron passage of S2 around Sgr A* ($t_0 = 2018.38$ and $P_0 = 16.046$ yr). Two solutions θ_1 and θ_2 disappear at the future pericenter passages in $t_d = 2034$ and 2050.

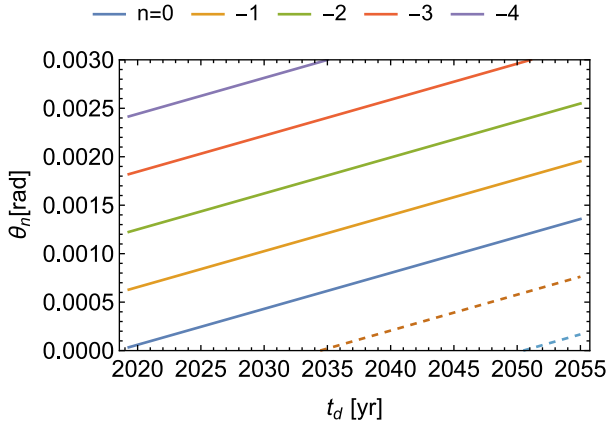


FIG. 4.— The opening angles θ_n for the receiving cones with $q=1$ (based on S2). New solutions appear at the future pericenter passages in $t_d = 2034$ and 2050.

hereafter. Then, as a function of the data taking epoch t_d , the formal solution to Eq. (7) is written as

$$\theta_n = \arccos[1 - fn - f(t_d - t_0)/P_0] \quad (11)$$

with $n > 0$.

In Fig. 3, we present the numerical results for $n = 1, \dots, 6$. We have the zero-points $\theta_n = 0$ at $t_d = t_n$ and the horizontal periodicity of $P_0 = 16.0$ yr. The shapes of the curves are identical and independent of P_0 and t_n . Note that, even with $n = 6$, we can cover the sky area with $\theta_6 = 0.08 \text{ rad} \sim 5^\circ$. For a reference, in Fig. 4, we also plot the results for $q = 1$. As shown in Eqs. (9) and (10), they are much smaller than those in Fig. 3 for $q = 0$.

It is important to recall that, only by precisely measuring the three parameters l_H , t_0 and P_0 , we can evaluate the opening angle θ_n for the signal reception and transmission. Then, we can simply access to the coordinated signaling scheme without prior communication. This is the major advantage of the scheme.

In Eq. (5), we put nP_0 for the next n rotation periods. If this estimation has a relative error smaller than that of the distance

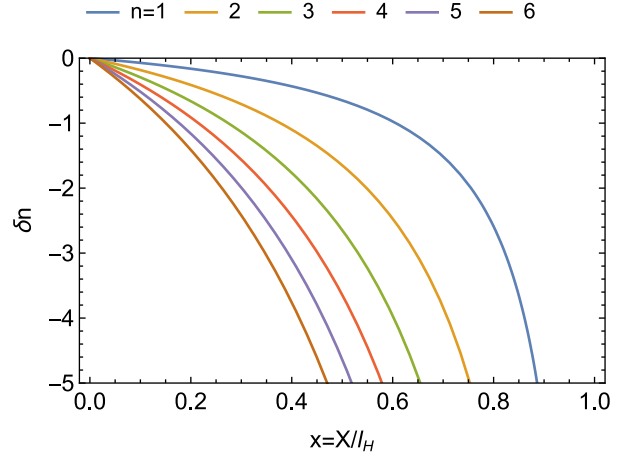


FIG. 5.— The rotation cycle difference δn of S2 observed by the Earth and a sender S at the distance X (see Fig. 1). We set our observational epoch at $t_d = 2024.000$ and the difference $\delta n = 5$ corresponds to the time difference of ~ 80 yr.

$\Delta l_H/l_H$, the width for each receiving circle $\Delta\theta_n$ is given as

$$\Delta\theta_n \sim \theta_n \frac{\Delta l_H}{2l_H}, \quad (12)$$

corresponding to timing error of

$$\Delta t \sim nP_0 \frac{\Delta l_H}{l_H}. \quad (13)$$

For $n = 6$, we obtain $\Delta\theta_6 \sim 2 \times 10^{-4} \text{ rad} \sim 0.7'$, using the current measurement accuracy $\Delta l_H/l_H \sim 0.005$. We can compactify the search directions by more than a factor of 100.

Note that the pericenter distance of S2 is ~ 17 light-hours. In Eq. (7), this should be compared with Eq. (13) of $\sim 30n$ light-days. Therefore, for the accuracy limited by the distance error $\Delta l_H/l_H$, we will be able to safely ignore the positional difference between the massive black hole and the pericenter of S2 (even considering the subtle general relativistic effects).

5. DEVIATION OF CLOCK

The scheme in the previous section relies on the regularity of the orbital motion of reference stars (in particular the periods between the pericenter passages). In reality, the orbital elements of stars in the nuclear star clusters will be gradually out of order, mainly by gravitational interaction with neighboring stars (see, e.g. Merritt 2013). Using the energy relaxation time $T_{\text{rel}} (\sim 10^{10} \text{ yr}$ for S2; see, e.g. Genzel et al. 2010) for the variation of the semimajor axis, we crudely estimate the period fluctuation $\Delta P \sim (T/T_{\text{rel}})^{1/2} P$ in the time interval T . For $T \sim 100 \text{ yr}$ (corresponding to $n \sim 6$), we have $\Delta P/P \sim 10^{-4}$, which is smaller than the current distance error $\Delta l_H/l_H \sim 5 \times 10^{-3}$. Given the chaotic nature of the orbital dynamics and probable existence of dark objects (e.g. stellar mass black holes), it would be difficult to beforehand correct the relaxation effects at high precision.

In any case, it would be reasonable for involved civilizations to calibrate the reference times t_n in Eq. (6) for the signaling, based on the actual data of the recent pericenter passages. Here, in Fig. 1, let us consider a signal transmission from the sender S to us (H) under the concurrent scheme. We should notice that, even with respect to the common S2 clock, the observed orbital phase at the signal transmission (by S) is

different from that at the signal reception (by H). Considering the long-term deviation of the S2 clock, we would like to have a small gap for the intervening orbital cycles. Here, we evaluate the cycle gap δn in a stepwise manner. We put the transmission time at the sender S by t_S and its distance from the Galactic center by l_S . By comparing the time difference back at the Galactic center (namely $t_S - l_S/c$ for the sender and $t_d - l_H/c$ for us), the cycle gap δn is formally given as

$$\delta n = \frac{(t_S - l_S/c) - (t_d - l_H/c)}{P_0}. \quad (14)$$

This expression is valid also for the choice $q = 1$. Next we apply this formal expression to the sender S on the propagation line in Fig. 1 at the distance X . The sending time t_S of S is given by

$$t_S = t_d - X/c, \quad (15)$$

and its Galactic radius becomes

$$l_S = \sqrt{l_H^2 + X^2 - 2l_H X \cos \theta_n}. \quad (16)$$

Plugging in these expressions to Eq. (14), we can evaluate the cycle difference δn between the sender S and us, as a function of X and our observational time t_d . Geometrically speaking, the numerator of Eq. (14) is the same as the time difference $[\text{HR} - (\text{CR} + \text{CH})]/c$ (see Fig. 1). For example, we have $\sim l_H \theta_n / c \sim 1300(\theta_n / 0.05 \text{ rad}) \text{ yr}$ for a civilization at the closest approach C.

In Fig. 5, we present the numerical results, introducing the normalized distance $x \equiv X/l_H$ and fixing $t_d = 2024.00$. Toward the sky direction around the Galactic center, we can keep $\delta n \lesssim 5$ to a significant depth $x \lesssim 0.5$ along the transmission lines, and the relaxation effects would be relatively unimportant for the signals from these civilizations. Even specifically, for the $n = 3$ sequence, to keep the observed time difference $P_0 \delta n$ less than 80 yr, the target civilization should be closer than $0.7 \times 8.3 = 5.8 \text{ kpc}$.

Meanwhile, by observing the consecutive pericenter passages, we can directly examine the variation of the orbital periods. For S2, we will have the next pericenter passage around $t_0 + P_0 = t_1 = 2034.38$ and will make extensive observation for studying various effects including relativity. Shortly before the next pericenter passage at t_1 , we have the condition $\theta_1 \sim 0$ (see Fig. 3) and can cover the depth $X \sim 1$. The observed period variation will enable us to partly estimate the valid depth X of the target civilizations. If the prospect for the $q = 0$ sequence is pessimistic, we could put more weight to the $q = 1$ sequence, which has smaller opening angles θ_n and is less affected by the long-term orbital perturbation.

Other short-period stars such as S4711 (Peißker et al. 2022) can also provide us with insights on the orbital perturbation. Note that the two-body relaxation time T_{rel} will be longer for a smaller semi-major axis (Genzel et al. 2010; Merritt 2013).

We should also notice that, in contrast to situation of a sender, a receiver has temporal flexibility at data analysis. For example, in 2036, based on the updated information of S2's pericenter passage in 2034, we can reanalyze the radio data taken, e.g. at $t_d = 2024.00$.

6. DISCUSSION

For concreteness, we have regarded the prominent star S2 as the common reference clock. As stated before, it will be valuable to examine possibilities of other objects, from the view of the Schelling point. Meanwhile, we might find a peculiar signal in a blind ETI search around the Galactic center

direction. Then, we can posteriori solve n for Eq. (7), using the timing parameters (t_0, P_0) associated with a small number of prominent reference objects including S2. If the solution n is close to an integer, it may be worth considering to make a deeper search to the incoming direction, after waiting for one orbital period P_0 of the corresponding reference object.

The distribution function for the durations of technologically advanced civilizations is totally uncertain. It is also difficult to assess the outlook of ours (see, e.g. Gott 1993). In the present scheme with S2, intentional signals can be repeatedly transmitted and scanned in a short period $P_0 = 16 \text{ yr}$. This might be advantageous for many Galactic civilizations, in contrast to a much longer scanning interval (e.g. $\gtrsim 10^4 \text{ yr}$ with binary neutron star mergers as discussed in Seto 2019).

So far, we have not examined relativistic effects to our simplified proposal. In the appendix, we discuss some corrections such as the aberration of light. While more detailed studies might be required before the actual application of our method, we expect that, for a relatively small n (e.g. $\lesssim 10$), the distance error $\Delta l_H / l_H \sim 0.005$ will currently limit our precision (except for the deviation of the clock). In the future, we might need to deal with corrections (including those in the appendix) to improve the total precision, using, e.g. Galactic models. Some of such effects will share similarities to high-precision measurements including astrometry (GRAVITY Collaboration et al. 2019, 2021). For the present scheme, we should also appropriately take into account the Schelling point argument, if necessary.

7. SUMMARY

The Galactic center is a conspicuous place in our Galaxy, and, relatedly, ETI signals have been search around its direction. Many stars nearly regularly orbit around the massive black hole there. Thanks to the enormous mass of the black hole, we can determine the distance l_H to the Galactic center at an exceptional precision ($\Delta l_H / l_H \sim 0.005$), despite the remoteness $l_H \sim 8.3 \text{ kpc}$.

The pericenter passages of a prominent object such as S2 will be a plausible option for the reference epoch, from the view of the Schelling point. Then, with the three locally measured parameters (l_H, t_0, P_0) , individual civilizations can determine the sending and receiving directions and access to the concurrent signaling scheme without prior communication. Considering the simplicity and usefulness, this scheme might be at a Schelling point in the strategy space of the interstellar signaling.

If S2 is really being used as a reference clock, our search directions are concentric circles centered by Sgr A*. The circles are continuously shrinking with the period of $P_0 \sim 16 \text{ yr}$ (see Fig. 3). With our present measurement precision $\Delta l_H / l_H \sim 0.005$, the width of each circle is $\sim 1'$, and we can compress the search sky directions by more than a factor of 100.

ACKNOWLEDGMENTS

The author would like to thank the referee for useful comments to improve the manuscript.

APPENDIX

RELATIVISTIC CORRECTIONS

So far, we have discussed the signaling scheme in a flat space-time, ignoring motions of senders and receivers. Here we briefly estimate some of the relevant corrections.

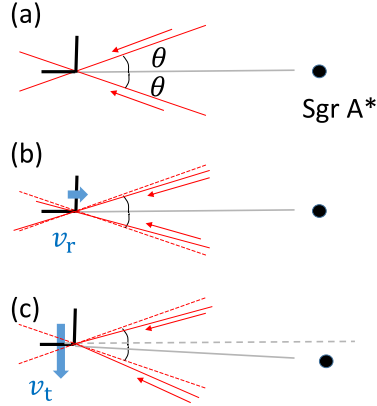


FIG. A6.— Aberration effects on the receiving cones due to the radial and tangential velocities. Frame (a) is at rest frame in the Galaxy. Frame (b) has the radial velocity v_r (toward Sgr A*) and the opening angle of its receiving cone (shown with the solid lines) shrinks, compared with the original one (the dashed lines). Frame (c) has the transverse velocity v_t relative to (a). In frame (c), the apparent sky direction of the Sgr A* and those of the receiving cone are similarly affected, and the net deviations are evaluated in Eq. (A2).

For our scheme, the simplest Galaxy-wide frame will be the rest frame relative to the Galactic center (more straightforwardly Sgr A*; see also Reid & Brunthaler 2020). This frame will be preferable also from the Schelling point. To discuss the magnitudes of the aberration effects caused by the radial and tangential velocities of the solar system, we consider the three frames (a), (b) and (c) at the position of the solar system (see Fig. 6). Frame (a) is at rest in the Galaxy (excluding the Galactic rotation velocity from the standard frame of rest Binney & Merrifield 1998). Relative to frame (a), frame (b) has the radial velocity $v_r \sim 10 \text{ km s}^{-1}$ (toward Sgr A*) and the frame (c) has the tangential velocity $v_t \sim 230 \text{ km s}^{-1}$ (Binney & Merrifield 1998) dominated by the Galactic rotation velocity. We apply the formula for the aberration angle (see e.g. Eq. (5.7) in Landau & Lifshitz 1975)

$$\delta\phi = \beta \sin\phi \quad (\text{A1})$$

with the angle ϕ between the incoming photon and the velocity of a moving frame ($\beta = v/c$, v : the magnitude of the velocity). This expression is valid for $\delta\phi \ll 1$ and $\beta \ll 1$.

In the second frame (b) shown in the middle panel of Fig. 6, the opening angle $\theta (\ll 1)$ of the receiving cone changes by $\beta_r \theta \sim 3 \times 10^{-6} (\theta/0.1 \text{ rad})$ (setting $\phi = \theta$ and $\beta = \beta_r = v_r/c$ in Eq. (A1)). This correction is much smaller than the uncertainty (12) associated with distance error Δl_H . We should notice that, due to the Doppler effect, in the frame (b), the observed orbital period becomes $(1 - \beta_r)$ times smaller than that in the original frame (a). With this modified period, for the scheme with $q = 0$, the estimated target angle θ is shrunk by a factor $\sim (1 - \beta_r/2) \neq (1 - \beta_r)$ (see, e.g. Eq. (9)). Therefore, unlike the case with $q = 1$, the correction for the radial velocity v_r cannot be automatically canceled by using the observed blueshifted orbital period.

Next we consider the third frame (c), which has the transverse velocity $v_t (= c\beta_t)$ relative to the frame (a) (see Fig. 6). For applying Eq. (A1), we evaluate the angles ϕ to the relevant directions. As shown in the upper panel of Fig. 6, in the frame (a), Sgr A* is at $\phi = \pi/2$, and, its receiving cone is in the range $\phi \in [\pi/2 - \theta, \pi/2 + \theta]$. In the moving frame (c), the three directions $\phi = \pi/2, \pi/2 \pm \theta$ are deformed as shown in the solid lines in the bottom panel, following Eq. (A1). Relative to the apparent direction of Sgr A*, the receiving cone has the maximum deformation

$$|\delta\phi_{\pi/2 \pm \theta} - \delta\phi_{\pi/2}| \sim \frac{\beta_t \theta^2}{2} \sim 10^{-5} \left(\frac{\theta}{0.1 \text{ rad}} \right)^2, \quad (\text{A2})$$

which is also smaller than the uncertainty (12) originating from the distance error Δl_H .

In our study, we studied propagation of photons in a flat space-time, without considering the Galactic potential. Associated with the path length difference in the context of Sec. 5 (e.g. $\delta l = \text{RS} + \text{SH} - \text{HR}$ in Fig. 1), we actually have a relativistic time correction (Shapiro time delay). We can roughly estimate its magnitude by

$$\frac{\beta^2 \delta l}{c} \sim 1 \left(\frac{\delta l}{1 \text{ kpc}} \right) \text{ day} \quad (\text{A3})$$

with the factor β for the Galactic rotation velocity $200 - 300 \text{ km s}^{-1}$ (see also Fig. 1 in Desai & Kahya 2016). This correction will be smaller than the uncertainty ~ 30 days, corresponding to the distance error Δl_H (see the paragraph after Eq. (12)).

REFERENCES

- Abbott, R., Abbott, T. D., Abraham, S., et al. 2021, *ApJ*, 913, L7.
Amaro-Seoane, P., Audley, H., Babak, S., et al. 2017, arXiv:1702.00786
Binney, J. & Merrifield, M. 1998, *Galactic astronomy* Princeton, NJ : Princeton University Press, 1998.
Bland-Hawthorn, J. & Gerhard, O. 2016, *ARA&A*, 54, 529.
Cocconi, G. & Morrison, P. 1959, *Nature*, 184, 844.
Desai, S. & Kahya, E. O. 2016, *Modern Physics Letters A*, 31, 1650083.
Drake, F. D. 1961, *Physics Today*, 14, 40
Eckart, A. & Genzel, R. 1996, *Nature*, 383, 415.
Gajjar, V., Perez, K. I., Siemion, A. P. V., et al. 2021, *AJ*, 162, 33.
Genzel, R., Eisenhauer, F., & Gillessen, S. 2010, *Reviews of Modern Physics*, 82, 3121.
Ghez, A. M., Duchêne, G., Matthews, K., et al. 2003, *ApJ*, 586, L127.
Gott, J. R. 1993, *Nature*, 363, 315.
GRAVITY Collaboration, Abuter, R., Amorim, A., et al. 2019, *A&A*, 625, L10.
GRAVITY Collaboration, Abuter, R., Amorim, A., et al. 2021, *A&A*, 647, A59.
Kaplan, D. L., Chatterjee, S., Gaensler, B. M., et al. 2008, *ApJ*, 677, 1201.
Kipping, D. M. & Teachey, A. 2016, *MNRAS*, 459, 1233.
Landau, L. D. & Lifshitz, E. M. 1975, *Course of theoretical physics - Pergamon International Library of Science, Technology, Engineering and Social Studies*, Oxford: Pergamon Press, 1975, 4th rev.engl.ed.
Lingam, M., & Loeb, A. 2021, *Life in the Cosmos: From Biosignatures to Technosignatures* (Cambridge, Massachusetts: Harvard University Press)
Makovetskii, P. V. 1980, *Icarus*, 41, 178.
McLaughlin, W. I. 1977, *Icarus*, 32, 464.
Merritt, D. 2013, *Dynamics and Evolution of Galactic Nuclei*, Princeton: Princeton University Press, 2013
Nilipour, A., Davenport, J. R. A., Croft, S., et al. 2023, *AJ*, 166, 79.
Nishino, Y., & Seto, N. 2018, *ApJ*, 862, L21
Pace, G. W. & Walker, J. C. G. 1975, *Nature*, 254, 400.
Peißker, F., Eckart, A., Zajaček, M., et al. 2022, *ApJ*, 933, 49.
Reid, M. J. & Brunthaler, A. 2020, *ApJ*, 892, 39.
Schelling, T. C. 1960, *The Strategy of Conflict* (Cambridge, Massachusetts: Harvard University Press)

- Schödel, R., Ott, T., Genzel, R., et al. 2002, *Nature*, 419, 694.
- Seto, N. 2019, *ApJ*, 875, L10
- Seto, N. 2021, *ApJ*, 917, 96.
- Shostak, G. S. & Tarter, J. 1985, *Acta Astronautica*, 12, 369.
- Siemion, A. P. V., Demorest, P., Korpela, E., et al. 2013, *ApJ*, 767, 94
- Suresh, A., Gajjar, V., Nagarajan, P., et al. 2023, *AJ*, 165, 255.
- Tarter, J. 2001, *Annual Review of Astronomy and Astrophysics*, 39, 511
- Tarter, J. C., Agrawal, A., Ackermann, R., et al. 2010, *Proc. SPIE*, 7819, 781902
- Tremblay, C. D., Price, D. C., & Tingay, S. J. 2022, *PASA*, 39, e008.
- Worden, S. P., Drew, J., Siemion, A., et al. 2017, *Acta Astronautica*, 139, 98.
- Wright, J. T. 2018, *Exoplanets and SETI*. In: Deeg H., Belmonte J. (eds) *Handbook of Exoplanets*. Springer
- Wright, J. T., Kanodia, S., & Lubar, E. 2018, *AJ*, 156, 260